J|A|C|S
ARTICLES
Published on Web 03/04/2004

Perturbation of Conjugation in Allylic Lithium Compounds Due to Stereochemical Control of Internal Lithium Coordination: Crystallography, NMR, and Calculational Studies

Gideon Fraenkel,* Albert Chow, Roland Fleischer, and Hua Liu

Contribution from the Department of Chemistry, The Ohio State University, 100 West 18th Avenue, Columbus, Ohio 43210-1185

Received June 20, 2003; E-mail: fraenkel@chemistry.ohio-state.edu

Abstract: Several allylic lithium compounds have been prepared with ligands tethered at C_2. These are with $(CH_3OCH_2CH_2)_2NCH_2-$, **6**, 1-TMS **5**, 1,3-bis(TMS) **8**, and 1,1,3-tris(TMS) **9**. Allylic lithiums with $(CH_3OCH_2CH_2)_2NCH_2C(CH_3)_2-$, are **10**, 1-TMS **11**, and 1,3-bis(TMS), **12** compounds with $-C(CH_3)_2CH_2N$-((*S*)-(2-methoxymethyl)-pyrrolidino) at C_2 **13**, 1-TMS **14**, and 1,3-bis(TMS) **15**. In the solid state, **8**−**10** and **12** are monomers, **6** and **13** are Li-bridged dimers, and **5** and **7** are polymers. In solution (NMR data), **5**, **7**−**12**, **14**, and **15** are monmeric, and **6** is a dimer. All samples show lithium to be closest to one of the terminal allyl carbons in the crystal structures and to exhibit one-bond $^{13}C-^{7}Li$ or $^{13}C_1-^{7}Li$ spin coupling, for the former typically ca. 3 Hz and for the latter 6−8 Hz. In every structure, the C_1-C_2 allyl bond is longer than the C_2-C_3 bond, and both lie between those for solvated delocalized and unsolvated localized allylic lithium compounds, respectively, as is also the case for the terminal allyl ^{13}C NMR shifts. Lithium lies 40−70° off the axis perpendicular to the allyl plane at C_1. These effects are variable, so the trend is that the differences between the C_1-C_2 and C_2-C_3 bond lengths, $^{13}\delta_3-^{13}\delta_1$ values, and the $^{13}C_1-^{7}Li$ or $^{13}C-^{6}Li$ coupling constants all increase with decreasing values of the torsional angle that C_1-Li makes with respect to the allyl plane.

In the solid state, all internal ligands are fully coordinated to lithium and none of the X-ray structures incorporate solvent. Also, in the solid-state monomers **8**−**10** and **12**, Li lies near the center of one face of a trigonal pyramid with two methoxy oxygens and nitrogen at its corners. Nitrogen occupies the apex.

The above results support a variable degree of delocalization in the allylic moiety due to the proximity of lithium to one of the terminal allyl carbons. The relative contribution of ionic and covalent interactions to the C−Li bond have yet to be determined. The ligand tether constrains the stereochemistry of lithium coordination, thus stabilizing these otherwise abberant structures.

Dynamics of inversion at lithium-bound carbon obtained from changes in the $^{13}C_1$ NMR line shapes due to the ligands gave $\Delta H^{\ddagger}$ values (kcal/mol) of 6.5 ± 0.4 and 15 ± 1.3 for ligand tethers of one and two carbons, respectively. Averaging of the $^{13}C_1-^{7}Li$ or $^{13}C_1-^{6}Li$ coupling constants observed with increasing temperature, which is due to bimolecular C_1-Li exchange, typically involves $\Delta H^{\ddagger}$ values of 12 ± 0.5 kcal/mol.

In the case of symmetrically substituted compounds **6**, **8**, **10**, **12**, and **15** ^{13}C NMR line shape changes provide the dynamics of lithium 1,3-sigmatropic shifts. The rates vary widely among the compounds studied, most likely due to steric effects.

Allylic lithium compounds are among the simplest potentially conjugated carbanionic species. As a result of extensive chemical,[1] spectroscopic,[2] crystallographic,[3] and calculational[4] studies, two principal types of structures have been identified. Solvated allylic compounds consist of contact ion-pairs. The anion is delocalized,[2,3] and coordinated Li^+ is sited on the axis perpendicular with and close to the center of the allyl plane, **1**[3]. By contrast, unsolvated allylic lithium compounds are regarded as

(1) (a) Wardell, J. L. *Comprehensive Organometallic Chemistry;* Wilkinson, G.; Stone, F. G. H.; Abel, E. W.; Eds.; Pergammon Press: Oxford, 1982; Vol. 7, p 97. (b) Seyferth, D.; Julia, T. F. *J. Organomet. Chem.* **1967**, *8*, C13. (c) Schlosser, M.; Stahle, N. *Angew. Chem.* **1980**, *92*, 477. (d) Stahle, M.; Schlosser, M. *J. Organomet. Chem.* **1981**, *220*, 277. (e) Neugebauer, W.; Schleyer, P. v. R. *J. Organomet. Chem.* **1980**, *198*, C1. (f) Brownstein, S.; Bywater, S.; Worsfold, D. J. *J. Organomet. Chem.* **1980**, *199*, 1. (g) Günther, H. *Encyclopedia of NMR* **1996**, *5*, 2807.

(2) (a) West, P.; Purmort, J. I.; McKinley, S. V. *J. Am. Chem. Soc.* **1968**, *90*, 797. (b) O'Brian, D. H.; Hart, A. J.; Russell, C. R. *J. Am. Chem. Soc.* **1975**, *97*, 4410. (c) Benn, R.; Rufinska, A. *J. Organomet. Chem.* **1982**, *239*, C19. (d) Bates, R. B.; Beavers, W. *J. Am. Chem. Soc.* **1974**, *96*, 5001. (e) Dolinskaya, E. R.; Poddabnyi, I. Ya.; Tseretech, I. Yu. *Dokl. Akad. Nauk. SSSR* **1970**, *191*, 802. (f) Thompson, T. B.; Ford, W. T. *J. Am. Chem. Soc.* **1974**, *101*, 5459. (g) Günther, H. *J. Brazil Chem. Soc.* **1999**, *10*, 241.

(3) (a) Koster, H.; Weiss, E. *Chem. Ber.* **1982**, *115*, 3422. (b) Schumann, U.; Weiss, E.; Dietrich, H.; Mahdi, W. *J. Organomet. Chem.* **1987**, *322*, 299. (c) Sebastian, J. F.; Grunwell, J. R.; Hsu, B. *J. Organomet. Chem.* **1974**, *78*, C1. (d) Boche, G.; Etzrodt, H.; Marsch, M.; Massa, H.; Baum, G.; Dietrich, H.; Mahdi, W. *Angew. Chem. 1986*, 98, 84. (e) Boche, G.; Fraenkel, G.; Cabral, J.; Harms, K.; Eikema-Hommes, N. J. P. Van.; Lorenz, J.; Marsch, M.; Schleyer, P. v. R. *J. Am. Chem. Soc.* **1992**, *114*, 1562−1565.

(4) (a) Erusalimski, C. B.; Kormer, V. H. *Zh. Org. Khim.* **1984**, *20*, 208. (b) Tidwell, E. R.; Russell, B. R. *J. Organomet. Chem.* **1974**, *80*, 175. (c) Boche, G.; Decher, G. *J. Organomet. Chem.* **1983**, *259*, 31. (d) Clarke, T.; Jemmis, E. D.; Schleyer, P. v. R.; Binkley, J. S.; Pople, J. A. *J. Organomet. Chem.* **1978**, *150*, 1. (e) Clarke, T.; Rhode, C.; Schleyer, P. v. R. *Organometallics* **1983**, *2*, 1344. (f) Bushby, R. J.; Tytho, M. P. *J. Organomet. Chem.* **1984**, *270*, 265. (g) Pratt, L. M.; Khan, I. M. *J. Comput. Chem.* **1995**, *16*, 1070. (h) Eikemma-Hommes, N. J. R. Van; Bühl, M.; Schleyer, P. v. R. *J. Organomet. Chem.* **1991**, *409*, 307−320.

localized species since their NMR spectra so closely resemble those of alkenes;[5] see **2a** and **2b**[5]. Until recently, structures that lie between **1** and **2** have not been recognized.

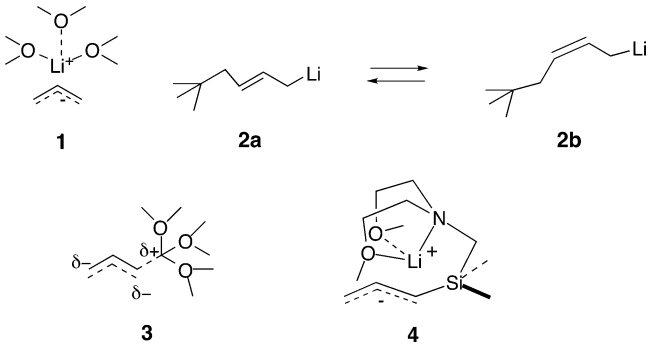

Our low-temperature NMR line shape analysis of solvated allylic lithium compounds has revealed the dynamics of a rich variety of fast molecular reorganization processes at equilibrium.[6] These include rotation around the C−C allyl bonds, transfer of coordinated lithium between faces of the plane (inversion), rotation of coordinated lithium on one side of the allyl plane, first-order reversible lithium ligand dissociation, and bimolecular lithium ligand exchange.

In experiments to slow these fast reorientational processes and thus facilitate the study of ion-pair structure, we encapsulated Li^+ in an allylic lithium compound by coordinating it to an attached ligand.[7] Using such an approach, we determined the first structure of an internally solvated ion-pair, **4**, using NMR methods.[7] Subsequently, we prepared several allylic lithium compounds with the pendant ligand attached to the center carbon of the allylic moiety.[8a−c] By contrast to **4**, these new compounds (see for example **5**) were not ion-paired salts. Their terminal allyl ^{13}C NMR shifts all lie between those for **1** and **2**.[8] They all displayed hitherto unprecedented spin coupling in an allylic lithium compound between one of the ^{13}C termini and ^6Li, indicating a small detectable degree of C−Li covalence. We proposed that the ligand tether in these compounds is too short to place lithium on the axis normal to the center of the allyl plane, as is the case in the delocalized structures, **1**. Instead, the ligand tether sites lithium off the axis perpendicular to the allyl plane at C_1. This restricts the stereochemistry of lithium coordination. The proximity of lithium to C_1 induces partial localization of the allylic moiety.[8b,c]

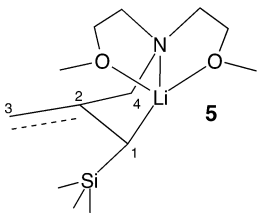

Compounds such as **5** also displayed interesting fast reorganization processes at equilibrium such as inversion at lithium-bound carbon, bimolecular C_1−Li exchange, and 1,3 lithium sigmatropic shifts.[8b,c]

Given that internal coordination of an otherwise delocalized organolithium compound can perturb its electronic structure, it is of interest to investigate the extent of the above-described effects: Is the degree of delocalization of our allylic lithium compounds continuously variable? How does this change with the length of the ligand tether and the nature of substitution on the allyl moiety? Clearly, quantitative structural information is required.

Herein we report crystal structures for several of these internally solvated allylic lithium compounds together with some new NMR data that provide unusual insight into dynamic behavior. These X-ray crystallographic results confirm in quantitative fashion the qualitative conclusions we have made, which are based on the results of our NMR studies. We show below how changes among the structural parameters correlate with trends among the NMR data and how the degree of delocalization in these internally solvated allylic lithium compounds is, in fact, continuously variable.

Results and Discussion

New crystallographic and NMR data are herein reported on **5** (see above) and on **6**−**15** (listed in Table 1 with ^{13}C NMR shifts).

The preparations of starting materials, not previously published, are outlined in the reactions **16** to **17**, **18** to **19**, **18** to **20**, **21** to **22** to **23**, **23** to **24**, and **24** to **25** (Scheme 1).

NMR data are reported herein for compounds **6**, **9**−**12**, **14**, and **15** (see Table 1). The samples were prepared by metalating compounds **16**−**20**, **24**, and **25**, respectively, with *n*-butyllithium in ether/hexane or THF/hexane. Then, solvents were replaced by THF-d_8 or diethyl-ether-d_{10}.

For the X-ray structure determinations, crystals of the allylic lithium compounds **5**−**10**, **12**, and **13** developed after metalation of their precursors using *n*-butyllithium in hexanes.

Salient Features of the Crystallographic Data. The crystallographic structures of compounds **5**−**10**, **12**, and **13** correlate with the NMR data. These compounds are monomers in the solid state except for **6** and **13**, which are lithium-bridged dimers, and **5** and **7** are polymers in the solid state. A Hirschfeld rigid bond analysis of our data,[9a] part of the PLATON software package,[9b] revealed nothing out of the ordinary among the thermal parameters. Selected structural and NMR parameters are listed in Table 2.

All the crystallographic structures exhibit full coordination of the pendant ligand to lithium and localized C−Li bonding. The crystal structure of a typical internally solvated monomer, compound **8**, is shown in Figure 1. Specific details of structure and bonding are outlined in the following sections.

Bond Lengths and Substitution. In all the crystal structures reported herein, C_1 C_2, C_3, and C_4 are coplanar. The numbering is indicated around structure **5**. Where a terminal allyl carbon

(5) (a) Fraenkel, G.; Halasa, A. F.; Mochel, V.; Stumpe, R.; Tate, D. *J. Org. Chem.* **1985**, *50*, 4563−4565. (b) Glaze, W. H.; Jones. P. C. *J. Chem. Soc.* **1969**, 1434. (c) Glaze, W. H.; Hanicac, J. E.; Moore, M. L.; Chandpuri, J. *J. Organomet. Chem.* **1972**, *44*, 39. (d) Glaze, W. H.; Hanicac, J. E.; Chandpuri, J.; Moore, M. L.; Duncan, D. P. *J. Organomet. Chem*. **1973**, *51*, 13.

(6) (a) Fraenkel, G.; Chow, A.; Winchester, W. R. *J. Am. Chem. Soc*. **1990**, *112*, 1382−1386. (b) Fraenkel, G.; Winchester, W. A.; Chow, A. *J. Am. Chem. Soc.* **1990**, *112*, 2582−2585. (c) Fraenkel, G.; Cabral, J. A. *J. Am. Chem. Soc.* **1993**, *115*, 1551−1557. (d) Fraenkel, G.; Cabral, J. *J. Am. Chem. Soc.* **1992**, *114*, 9007−9015. (e) Fraenkel, G.; Cabral, J.; Lanter, C.; Wang, J. *J. Am. Chem. Soc.* **1999**, *64*, 1302−1310.

(7) Fraenkel, G.; Cabral, J. A. *J. Am. Chem. Soc.* **1993**, *115*, 1551.

(8) (a) Fraenkel, G.; Qiu, F. *J. Am. Chem. Soc.* **1997**, *119*, 3571−3579. (b) Fraenkel, G.; Qiu, F. *J. Am. Chem. Soc.* **1996**, *118*, 5828−5829. (c) Fraenkel, G.; Duncan, J. H.; Wang, J. *J. Am. Chem. Soc.* **1999**, *121*, 432−443. (d) Fraenkel, G.; Martin, K. *J. Am. Chem. Soc.* **1995**, *117*, 10336−10344.

(9) (a) Hirschfeld, F. L. *Acta Crystallogr*. **1976**, *A32*, 239. (b) Spek, A. L. *J. Appl. Crystallogr*. **2003**, *36*, 7.

Table 1. Structures of Internally Solvated Allylic Lithium Compounds with ^{13}C NMR Shifts

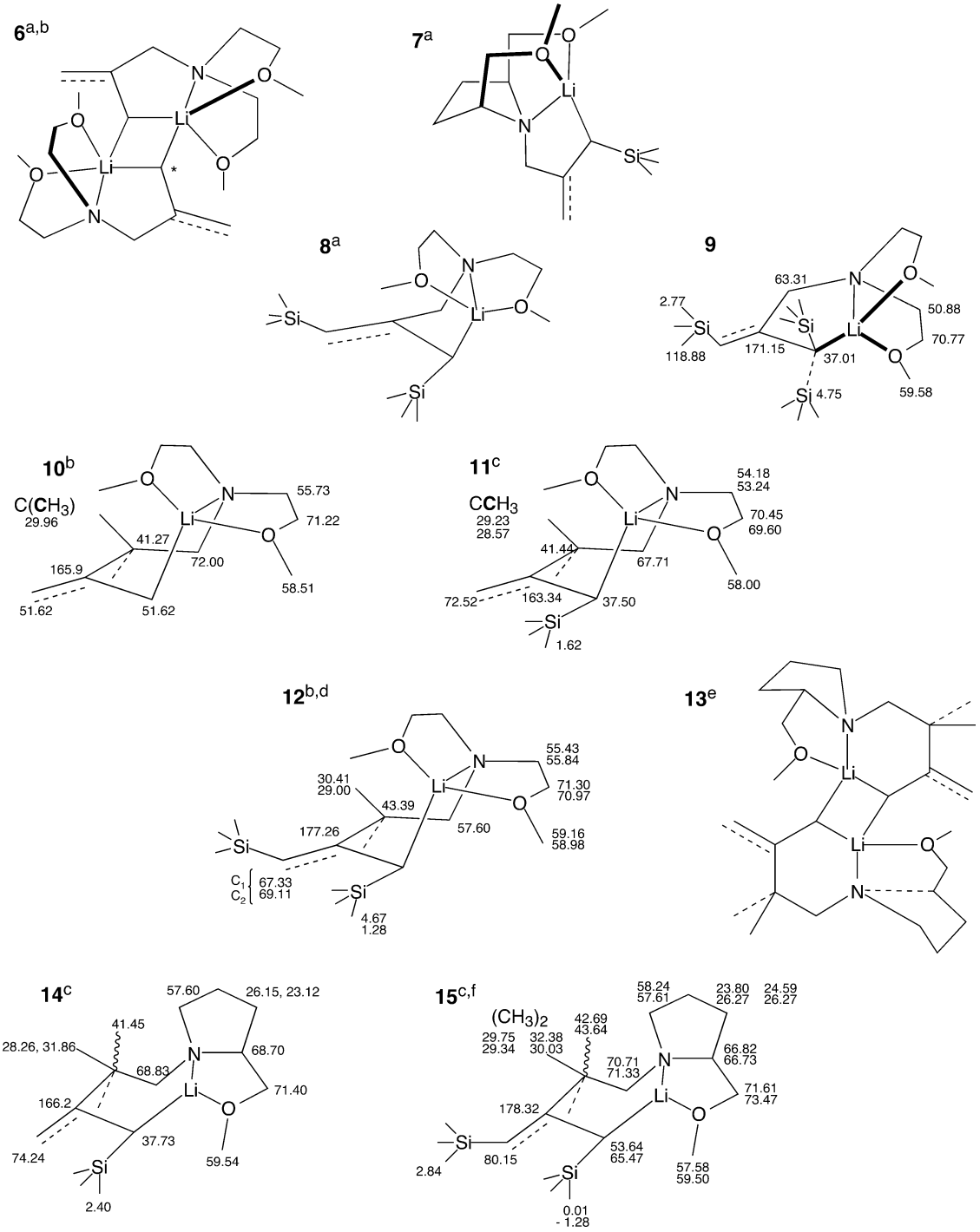

[a] NMR previously reported. [b] Subject to fast sigmatropic shift; see text. [c] Did not crystallize; [d] Two stereoisomers in a 1:1 ratio. [e] Insoluble. [f] Two stereoisomers in a 2:1 ratio; shift for major species is indicated by top value of each stack.

carries a single silyl substituent, the C−Si bond lies close to the allyl plane. In **9** with geminal silyl substituents at C_1, these lie well separated on opposite sides of the allyl plane (see Table 2).

The two allyl C−C bond lengths in simple externally solvated allylic lithium compounds are very similar,[3] as are also the terminal allyl ^{13}C NMR shifts.[2] By contrast, within each of the internally solvated allylic lithium compounds, both the allyl bond lengths and the terminal allyl ^{13}C shifts are significantly different (see Table 2). The values of these bond lengths and shifts lie between those of delocalized **1** and values for simple substituted alkenes, which we assume resemble the bond lengths of **2**. The localized allyl ^{13}C shifts of **2** are very similar to those of alkenes. The data for the compounds reported in this article indicate a trend for the chemical shift differences $^{13}\delta_3-{}^{13}\delta_1$ to increase with differences between the C_1-C_2 and C_2-C_3 bond lengths. These differences are largest for **9**, the allyl ^{13}C shifts and bond distances of which closely resemble those of an alkene. This is due to steric interactions associated with the geminal silyl substituents at C_1 (see specific details below).

Scheme 1 [a–i]

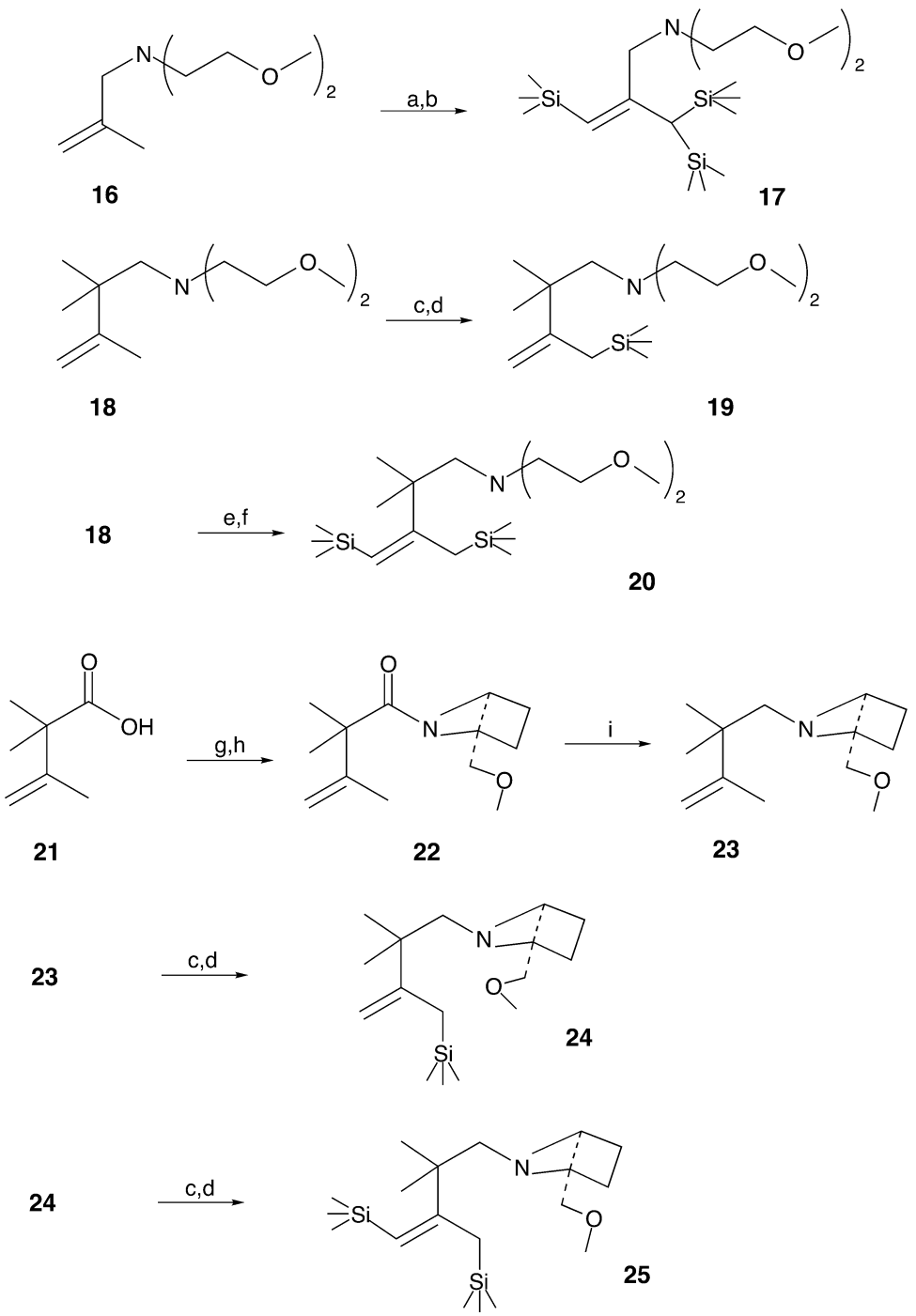

[a] *n*-BuLi 3 equiv, hexane/Et_2O, 0 °C; [b]TMSCl 3 equiv, −78 °C; [c]*n*-BuLi 1 equiv, hexane/Et_2O, 0 °C; [d]TMSCl 1 equiv, −78 °C; [e]*n*-BuLi 2 equiv, hexane/Et_2O, 0 °C; [f]TMSCl, 2 equiv, −78 °C; [g]$SOCl_2$, 85 °C; [h](*S*)-(+)-2-methoxymethylpyrrolidine; [i]LAH, THF, reflux.

The crystallographic structures of **5** and **7** are exceptions to the trend desribed above. These compounds are polymers in the solid state due to a fifth coordination between lithium and the terminal methylene carbon of a neighboring allylic lithium unit. As a consequence, the two allyl bond lengths C_1-C_2 and C_2-C_3 in these compounds are quite similar. Figure 2 illustrates this bonding arrangement in the crystal structure of compound **5**. However, the results of NMR studies show that, in solution, **5** and **7** appear to be monomers.[8a–c]

It is interesting that the average of the C_1-C_2 and C_2-C_3 bond lengths within each internally solvated allylic lithium compound is quite close to the average allylic C−C bond lengths in the corresponding externally solvated delocalized allylic lithium compound. For example, the average bond lengths for the unsubstituted internally solvated compounds **6** and **10**, 1.392 (2) and 1.396 (2) Å, respectively (see Table 2), compare closely to the 1.370 Å value reported for the allyllithium pentamethyldiethylenetriamine[3b] (PMDTA) complex, despite the fact that

Table 2. X-ray Structural and NMR Parameters of Internally Solvated Allylic Lithium Compounds (Note: M = Monomer, D = Dimer, P = Polymer; for Numbering See Structure **5**)

				bond lengths (Å)		^{13}C shifts		torsional angles[a]		
	solid	solution	J ^{13}C–Li (Hz)	C_1–C_2	C_2–C_3	C_1	C_3	Li–C_1–C_2–C^0_4	Si_1–C_1–C_2–C^0_4	Si_3–C_3–C_2–C^0_4
6	D	D	*b*	1.436(4)[c]	1.349(1)[c]	58.55[b]	58.55[b]	−50.12(0.03)[c]		
5	P	M	3.0 ^{6}Li	1.397(4)	1.361(4)	41.10	76.30	−55.27(0.25)	173.59(0.19)	
7	P	M	7.0 ^{7}Li	1.415(7)	1.351(8)	42.81	72.95	47.8(5)	179.6(4)	
8	M	M	6.1 ^{7}Li	1.431(3)	1.351(3)	54.12	78.10	52.97(0.2)	176.7(0.16)	−5.32(0.34)
9	M	M	15.9 ^{7}Li	1.494(7)	1.306(8)	37.01	118.88	−30.3(0.61)	82.03(0.58)[d] −142.37(0.48)[d]	−9.13(1.12)
10	M	M	*b*	1.426(2)	1.366(2)	51.62[b]	51.62[b]	73.46(0.14)		
11	*e*	M	8.1 ^{7}Li	*e*	*e*	37.50	72.52	*e*	*e*	
12	M	M	4.6 ^{7}Li[f] 4.1 ^{7}Li[f]	1.415(8)	1.368(20)	67.33[b]	69.11[b]	−90.9(3)	171.3(3)	15.1(7)
13	D	*g*	*g*	1.415(8)[c]	1.368(20)[c]	*g*	*g*	−103.58(3)[c]		
14	*e*	M	8.7 ^{7}Li	*e*	*e*	37.73	74.24	*e*	*e*	
15	*e*	M[h]	5.1 ^{7}Li	*e*	*e*	53.64[h] 65.47[h]	80.15[h] 80.15[h]	*e*	*e*	*e*

[a] Torsional angle with respect to allyl plane at C_2−C_4. [b] Exchange averaged. [c] Weighted average over two dimers. [d] Refers to 1,1-bis(TMS). [e] Did not crystallize. [f] Averaged values; see text. [g] Insoluble. [h] Two stereoisomers.

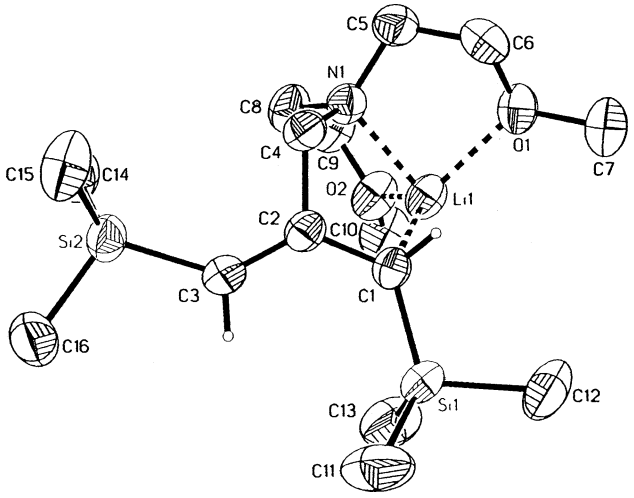

Figure 1. ORTEP diagram of compound **8** showing 50% thermal ellipsoids, and selected atoms are labeled. Hydrogen atoms have been omitted for clarity.

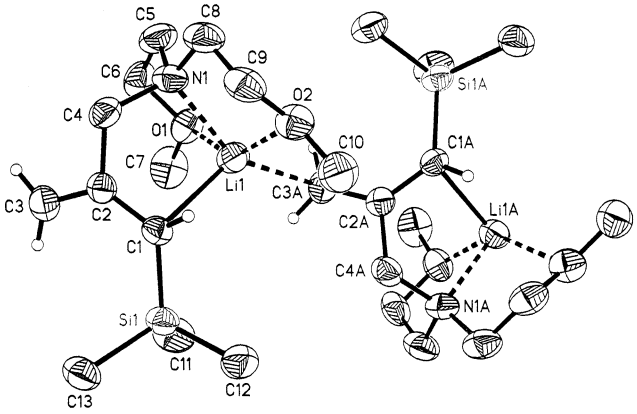

Figure 2. ORTEP of two units of **5** showing 50% thermal ellipsoids and selected atom labels. Hydrogen atoms have been omitted for clarity.

6 is a dimer while allyllithium·PMDTA and **10** are monomers. In similar fashion, the average allylic C−C bond length of 1.391 Å in internally solvated 1,3-disilyl **8** (see Table 2) is close to the corresponding value of 1.403 Å in externally solvated **26**.[3e]

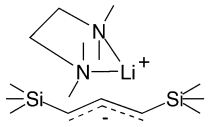

26

Site of Lithium. In delocalized externally solvated allylic lithium compounds, lithium lies perpendicularly on the axis to be close to the center of the allyl plane.[3] These compounds have not been reported to exhibit ^{13}C−^{7}Li or ^{13}C−^{6}Li spin coupling.[2] By contrast, X-ray crystallography of **6**−**10**, **12**, and **13** shows lithium to be closer to the terminus, defined as C_1, of the longer C−C allyl bond than to the other two allyl carbons. Note that almost all the solution ^{13}C NMR data for these internally solvated allylic lithium compounds show the more shielded of the allyl ^{13}C termini to be spin coupled to ^{6}Li or ^{7}Li. This matches the latter carbon to C_1 in the X-ray crystallographic data. Thus, X-ray crystallography and NMR together strongly support our proposal that these compounds are partially localized.[8a−c]

Further insight into these structures is provided by angular relationships. The Li−C_1−C_2 angle is typically around 90°, though the full range is between 70 and 100° (see Table 2). The dihedral angle that C_1−Li makes with respect to the allyl plane on the ligand side, Li−C_1−C_2−C_4, depends on the ligand tether as well as on substitution at the allyl termini. In compounds **5**−**8**, this torsional angle, Li−C_1−C_2−C_4, is close to 50°. All four compounds, **5**−**8**, incorporate a one-carbon ligand tether. Compound **6** is unsubstituted at the allyl termini, whereas in **5**, **7**, and **8** there is a single substituent at C_1 and the C_1−Si bond lies close to the allyl plane. By contrast, in **9**, also with a one-carbon ligand tether, there are *two silyl substituents at* C_1, which are well separated by 135° on opposite sides of the allyl plane. The lower Li−C_1−C_2−C_4 torsional angle of 30.03° minimizes potential steric interactions between the silyl substituents and the ligand. By contrast to compounds **5**−**8**, the longer two-carbon ligand tether in **10**, **12**, and **13** allows the Li−C_1−C_2−C_4 torsional angle to increase, respectively, to 73.46, 90.01, and 101° (see Table 2).

Lithium Coordination. The coordination geometry around lithium is unusual among these internally solvated allylic lithium compounds. In compounds that are monomers in the solid state, **8**−**10** and **12**, lithium lies close to the center of one face of a trigonal pyramid with C_1 and the two methoxy oxygens at its corners. Nitrogen occupies the apex (see Figure 3a). A similar

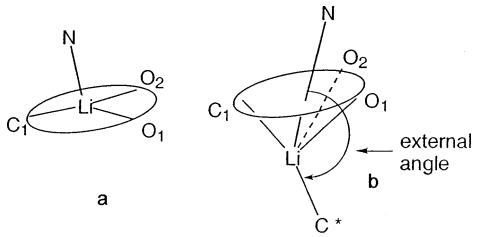

Figure 3. (a) Coordination around lithium in monomeric **8**−**10** and **12**. (b) Coordination around lithium in polymeric **5** and **7**.

Table 3. Internally Solvated Allylic Lithium Compounds: Bond Distances around Lithium, Å

	N–Li	Li–C_1	Li–O_1	Li–O_2	Li–C_3*
6[a]	2.147(7)	2.317(8)	2.087(7)	2.15(7)	2.382(7)
5[b]	2.138(5)	2.316(5)	2.145(5)	2.375(5)	2.442(5)
7[b]	2.182(10)	2.515(11)	2.138(10)	2.117(10)	2.481(11)
8[c]	2.041(4)	2.186(4)	1.968(4)	2.035(4)	
9[c]	2.009(11)	2.171(12)	2.047(12)	2.012(11)	
10[c]	2.065(3)	2.158(3)	2.038(3)	2.002(3)	
12[c]	2.081(7)	2.220(8)	2.025(8)	2.025(7)	

[a] Dimer; see structure **6** weighted averages over two dimers. [b] Polymers, C_3* is C_3 of nearest neighbor unit; for numbering, see Figure 3b. [c] Monomers; see Figure 3a.

scheme applies to **5** and **7** with the exception that these compounds are polymerized in the solid state due to a fifth coordination from lithium to the allyl methylene carbon of a neighboring allylic lithium unit (see Figure 3b). Lithium lies 0.4 Å on the opposite side of nitrogen with respect to the $C_1-O_1-O_2$ plane within the resulting distorted trigonal bipyramid (see Figure 3b). Of the two C−Li bonds associated with **5**, C*−Li (external) at 2.442(5) Å is significantly longer than C−Li (internal) at 2.316(5) Å, whereas in **7** the corresponding bonds are of similar lengths, C_1−Li 2.515(11) Å (internal) and C*-Li 2.48 (11) Å (external). The two external angles N−Li−C* in **5** and **7** are, respectively 147.5 and 168.2° (see Figure 3b and Tables 2−4).

Influence of Reorganization Dynamics on NMR Spectra. Comparisons of X-ray crystallographic and NMR data for our internally solvated allylic lithium compounds indicate that in most cases the solid- and solution-state structures are very similar. On the basis of our previous NMR studies of **5**, **7**, and **8** and the crystallographic results reported herein, one would expect compounds **6** and **9**−**15** to all exhibit $^{13}C-^{6}Li$ or $^{13}C-^{7}Li$ spin coupling and that, in the ^{13}C NMR of each compound, all the carbons should be magnetically nonequivalent. That this is not always the case is largely due to the operation of one or more dynamic effects. Thus, as seen below, NMR alone is inadequate to reveal structures and unravel dynamic behavior for several compounds described herein. Below, we first summarize the influence of different dynamic phenomena on the NMR of our internally solvated allylic lithium compounds. Then, by *combining* NMR and crystallographic data we will individually discuss and interpret the results for compounds **6**, **10**, **13**, **8**, **12**, **11**, and **14**, in the preceding order, in terms of their structures and the nature of their reorganization processes.

Inversion Dynamics. At low temperature (170 K), all carbons of the $N(CH_2CH_2OCH_3)_2$ pendant ligand in **5** are magnetically nonequivalent and the ^{13}C resonance for each of $\mathbf{C}H_3O$, $\mathbf{C}H_2O$, and $N\mathbf{C}H_2C$ consists of an equal doublet. When the temperature is increased above 170 K, these doublets progressively average to single lines at their respective centers.[8b] NMR line shape analysis of each of these averaging doublets gives rise to the same rate constants. This effect was ascribed to fast transfer of coordinated Li^+ between faces of the allyl plane, essentially inversion at C_1. This proposal was confirmed by similar ^{13}C NMR data obtained with an analogue of **5** using **27** ($X = (CH_3)_2SiCH_2CH_3$). The geminal silyl methyls in the latter compound are *diastereotopic* at 170 K and average with increasing temperature above 170 K. Line shape analysis of the latter *methyl resonance* as well as the *ligand resonances* gave rise to the same rate constants.[8c] This also establishes that configurational inversion at C_1 in these compounds is a much faster process than inversion at nitrogen alone.

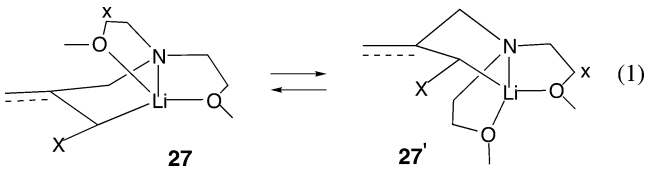

(1)

Typical $\Delta H^{\ddagger}$ values for inversion among internally solvated allylic lithium compounds are 6.5 ± 0.4 kcal/mol for a one-carbon tether and 15 ± 1.3 kcal/mol when the tether is two carbons long, as in compound **11** below (see Table 5).

Fast configurational inversion may also result from sigmatropic shifts in symmetrical compounds, which is discussed next.

1,3 Lithium Sigmatropic Shifts. We previously reported that on warming compound **8** between 260 and 330 K, the two trimethylsilyl ^{13}C resonances progressively average as do also the terminal allyl ^{13}C resonances.[8b] This is due to a fast 1,3 lithium sigmatropic shift (see eq 2). These shifts are a potential feature of the dynamic behavior of our symmetrically substituted and unsubstituted internally solvated allylic lithium compounds. In such latter cases, where the pendant ligand is $-N(CH_2CH_2OCH_3)_2$, the sigmatropic shift also brings about configurational inversion (see eq 2).

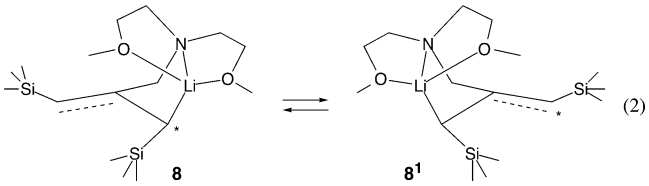

(2)

Details regarding the dynamics of sigmatropic shifts in compounds **6**, **10**, and **13** (unsubstituted) followed by **8**, **12**, and **15** (1,3-disubstituted) are outlined and discussed separately below. The rates of these sigmatropic shifts vary widely among the latter compounds.

$^{13}C-^{6}Li$ and $^{13}C-^{7}Li$ Spin Coupling and its Perturbation by the Dynamics of C−Li Exchange and ^{7}Li Relaxation. Most of the monomeric compounds described herein exhibit one-bond $^{13}C-^{7}Li$ or $^{13}C-^{6}Li$ spin coupling; typical coupling constants are 7.5 ± 0.5 and 2.8 ± 0.2 Hz,[8] respectively (see Table 2). These values are similar to those we have reported for one-bond ^{13}C−lithium coupling constants in internally solvated benzylic lithium compounds[8d] but rather smaller than those observed for one-bond $^{13}C-^{7}Li$ or $^{13}C-^{6}Li$ coupling constants in many different monomeric organolithium compounds, 41 Hz for the former and 15.5 Hz for the latter. It has been pointed out that one-bond $^{13}C-^{6}Li$ (or ^{7}Li) coupling constants should decrease with increasing $^{\delta-}C\cdots^{\partial+}Li$ dipole

Table 4. Internally Solvated Alllylic Lithium Compounds Lithium Coordination Angles (deg), Monomers unless Otherwise Noted

	O_1LiO_2	O_1LiC_1	$O_2L_1C_1$	N_1LiC_1	$NLiO_1$	$NLiO_2$		C_1*LiC_1	C_1*LiO_1	C_1*LiO_2
6[a]	114.2(2)	106.6(11)	131.2(11)	83.3(2)	79.3(4)	79.0(3)	**6**[a]	109.0(5)	97.6(1)	91.7(0)
5[b]	145.2(2)	104.7(2)	95.59	85.2(2)	80.2(2)	76.1(17)		C_3*LiC_1	C_3*LiO_1	C_3*LiO_2
7[b]	130.3(3)	112.4(4)	108.0(4)	81.1(3)	77.6(3)	81.4(4)	**5**[b]	127.3(2)	86.6(2)	100.1(2)
8	117.3(2)	129.8(2)	112.1(2)	88.7(2)	87.5(2)	84.1(2)	**7**[b]	110.7(4)	97.1(4)	94.4(4)
9[c]	102.8(5)	123.4(5)	132.5(5)	89.9(4)	85.1(4)	83.2(4)				
10[c]	119.78(12)	122.85(13)	115.9(12)	112.26(12)	84.38(9)	86.45(10)				
12[c]	100.5(3)	107.8(3)	149.6(4)	108.5(3)	84.8(3)	84.5(3)				

[a] Dimer; see structure **6**. [b] Polymer; C_3* is terminal allyl carbon of nearest neighbor; see Figure 3b. [c] Monomer; see Figure 3a.

Table 5. Quantitative and (Qualitative) Dynamic Behavior of Internally Solvated Allylic Lithium Compounds, Diethyl Ether-d_{10} Solution

	C–Li exchange		inversion		1,3 Li sigmatropic shift 250 K
compd	$\Delta H^{\ddagger}$ (kcal/mol)	ΔS (eu)	$\Delta H^{\ddagger}$	$\Delta S^{\ddagger}$	k_1 (s^{-1})
5	11± 0.5[a]	−6± 2[a]	8± 0.5[a]	−10± 3[a]	
6	(fast)[b]		(fast)[b]		8.8×10^{6} [c,d]
7	12[e]	−5± 2[e]	9± 0.5[e]	−7± 2[e]	
8					1.0
9	(slow)[f]				
10	(fast)[b]		(fast)[b]		1.4×10^{5} [c,g]
11	11 ± 0.5	−15 ± 4	15 ± 1	+2 ± 0.5	
12	(slow)[f]		(slow)[e]		$>10^{8}$
14	6 ± 0.3	−27 ± 5			
15	(slow)[f]				$<10^{-2}$

[a] Ref 8b. [b] Too fast to measure. [c] Estimated from line broadening, see text. [d] SD = ± 2.6×10^{5} s^{-1}. [e] Ref 8c. [f] Too slow to measure. [g] SD = ± 6.1×10^{4} s^{-1}.

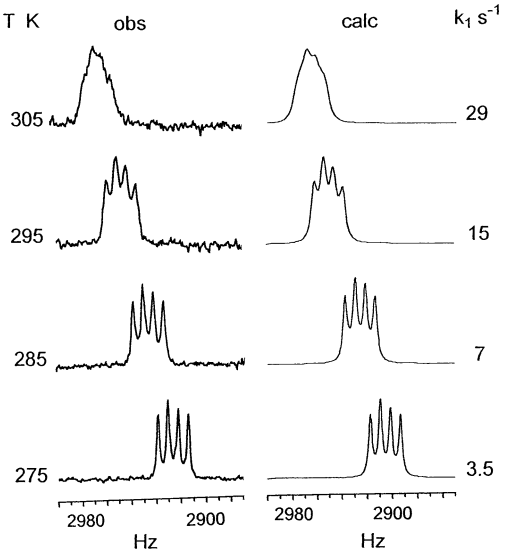

Figure 4. ^{13}C NMR (75.45 MHz) line shapes for **11**, ^{7}Li-bound ^{13}C (left) observed at different temperatures, and (right) calculated with a first-order rate constant. Dissymmetry is due to an impurity resonance below the starred peak. It was taken into account in the line shape calculation by addition of a fifth density matrix equation.[12]

moments.[10a] Further, a careful reading of the pioneering theoretical treatment of one-bond Fermi contact coupling by Ramsey, Karplus, and Grant[10b−d] leads to the conclusion that a small contribution of covalence to scalar coupling cannot be eliminated.

Two dynamic effects are responsible for averaging the $^{13}C-^{7}Li$ coupling in our internally solvated allylic lithium compounds. These are bimolecular C−Li exchanges, whose rate increases with temperature[8] and ^{7}Li electric quadrupole-induced relaxation.[11] The latter rate increases with decreasing temperature. In the case of $^{13}C-^{6}Li$ coupling, only bimolecular C−Li exchange averages this coupling since the quadrupole moment of ^{6}Li is too small to perturb the ^{13}C NMR of ^{6}Li bound ^{13}C.

The dynamics of bimolecular C−Li exchange can be determined if there is a temperature at which $^{13}C-^{7}Li$ or $^{13}C-^{6}Li$ spin coupling is *clearly resolved*. If when the sample is warmed the coupling is progressively averaged, this effect is exclusively due to bimolecular C−Li exchange.[8d,12,13] As far as the ^{13}C NMR of ^{7}Li-bound carbon is concerned, the monomeric exchanging system with ^{13}C in natural abundance is simulated as in eq 3.

$$^{13}C^{7}Li + {}^{12}C^{7}Li^{*} \rightleftarrows {}^{13}C^{7}Li^{*} + {}^{12}C^{7}Li \qquad (3)$$

Comparison of the experimental $^{13}C_1$ NMR spectrum with line shapes calculated to take account of the above exchange process, eq 3,[12,13] provides the second-order rate constants and the accompanying activation parameters for C−Li exchange. For example, in the case of **11** in diethyl ether-d_{10}, comparison of the ^{13}C line shapes for lithium-bound carbon shown in Figure 4 results in $\Delta H^{\ddagger}$ and $\Delta S^{\ddagger}$ for bimolecular C−Li exchange of, respectively, 11 ± 0.5 kcal/mol and −15 ± 4 eu (Table 5). In fact, all the allylic lithium compounds internally coordinated to the $N(CH_2CH_2OCH_3)_2$ ligand that we have studied show very similar activation parameters for C−Li exchange with $\Delta H^{\ddagger}$ = 11 to 12 kcal/mol (see Table 5). This may imply that decoordination of lithium to the pendant ligand is rate determining for C−Li exchange among these compounds. However, with a different ligand, as in **14**, $\Delta H^{\ddagger}$ for C−Li exchange is much lower at 6 ± 0.3 kcal/mol. By contrast, activation parameters for the other reorganization processes that these compounds undergo vary greatly among the different species we have investigated.[8a−c]

In several cases, for example **8**, progressive averaging of the $^{13}C-^{7}Li$ coupling constant is also observed on cooling the sample *below* the temperature at which this coupling is clearly resolved, 260 K. The character of these line shape changes is uniquely diagnostic of the operation of ^{7}Li nuclear electric quadrupole-induced relaxation, whose rate increases with decreasing temperature.[11] Note that depending on the relative rates of bimolecular C−Li exchange and ^{7}Li nuclear electric quadrupole-induced relaxation, there may not be a temperature at which $^{13}C-^{7}Li$ coupling is well resolved.[11]

(10) (a) Bartlett, R. J.; Del Bene, J. E.; Perera, S. A. B. *Structures and Mechanisms: from Ashes to Enzymes*; ACS Symposium Series 827; American Chemical Society: Washington, DC, 2002; pp 150−164 and references therein. (b) Ramsay, N. F. *Phys. Rev.* **1953**, *91*, 303. (c) Grant, D. M.; Litchman, W. M. *J. Am. Chem. Soc.* **1965**, *87*, 3994. (d) Litchman, W. M.; Grant, D. M. *J. Am. Chem. Soc.* **1967**, *89*, 2228. (e) Karplus, M.; Grant, D. M. *Proc. Nat. Acad. Sci. U.S.A.* **1959**, *45*, 1269.
(11) Fraenkel, G.; Subramanian, S.; Chow, A. *J. Am. Chem. Soc.* **1995**, *117*, 10336−10344.
(12) Kaplan, J. A.; Fraenkel, G. In *NMR of Chemically Exchanging Systems;* Academic Press: New York, 1980; Chapters 5 and 6.
(13) Ref 9, p 10341.

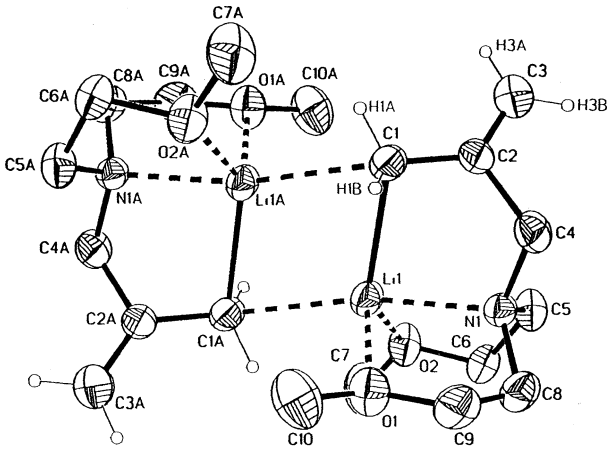

Figure 5. ORTEP of **6** showing 50% thermal ellipsoids. Selected atoms are labeled. Hydrogen atoms have been omitted for clarity.

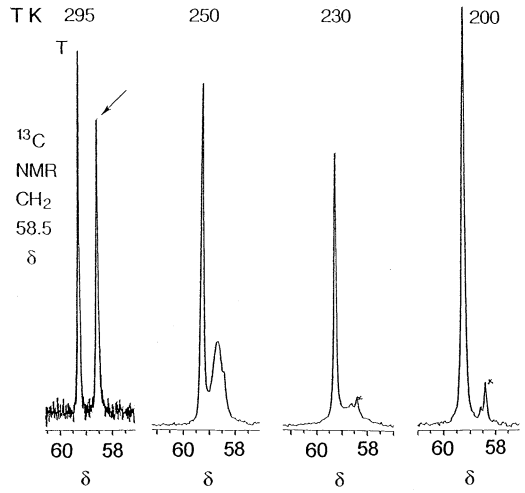

Figure 6. ^{13}C NMR (75.45 MHz) of **6** over the range 57−61 δ showing the temperature dependence of the ^{13}C resonance at 58.5 δ due to terminal allyl carbon; **C**H_3O resonance at 59.4 δ; star marks an impurity.

Compound 6. Carbon-13 NMR of **6** in diethyl ether-d_{10} solution at room temperature gave a single narrow resonance for the terminal allyl carbons at 58.55 δ. The two 2-methoxyethyl groups were magnetically equivalent, and ^{13}C−^{6}Li spin coupling was not observed. Similar spectra were obtained for solutions of **6** in benzene-d_6 and in toluene-d_8. At first, these results appeared to be consistent with a delocalized structure. However, X-ray crystallography showed **6** to be a lithium-bridged dimer in the solid state with *localized* C_1−*Li* bonding (see Figure 5). Determination of the freezing point of a solution of **6** in benzene showed **6** to be a dimer in benzene solution as well as in the solid state. At this point, ^{13}C NMR of **6** in diethyl ether was reinvestigated as a function of temperature. On cooling the sample below room temperature, the resonance we assigned to the terminal allyl carbons at 58.55 δ progressively broadened and disappeared into the baseline at 200 K (see Figure 6). In all other respects the spectrum remained unchanged throughout the entire temperature range 300−150 K. Resonances that could be assigned to the terminal allyl carbons were not detected between 200 and 150 K. Similar behavior was also observed using toluene-d_8 solutions of **6**. These results strongly imply that dimer **6** is the principal species present in benzene, toluene, and diethyl ether as well as in the solid state.

To account for the results described, above we would like to propose that dimer **6** is in rapid equilibrium with a low and undetectable concentration of monomer **28** (eq 4) and that the terminal allyl ^{13}C shifts in **6** are averaged by a fast 1,3 lithium sigmatropic shift that takes place in monomer **28** (see eq 5). Varying the concentration of **6** between 0.05 and 0.6 M did not change the appearance of this spectrum. Fast monomer−dimer interconversion (eq 4) would average the ^{13}C−^{7}Li or ^{13}C−^{6}Li coupling constants. In addition, the fast 1,3 lithium sigmatropic shift would invert the configuration of **28** and overall average the shifts between the two arms of each pendant ligand in **6** (see eq 5).

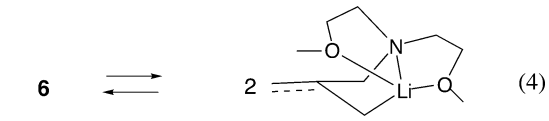

(4)

28

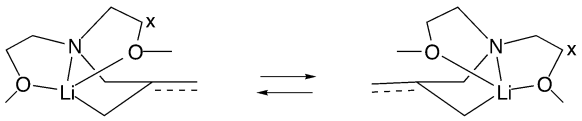

(5)

28 **28**[1]

Evidently, the 1,3 lithium sigmatropic shift (see eq 5) is still too fast at 150 K to allow observation of well resolved ^{13}C resonances for the terminal allyl carbons of **6**. However, a value for $\delta_3-\delta_1$ for **6** could be estimated via ab initio calculations using the Gaussian 98 programs.[14] Starting with its crystallographic parameters, compound **6** was geometry optimized at the RHF level of theory with basis set 6-31 G*. Frequency calculations were used to confirm that the optimized geometry corresponded to the minimum-energy configuration. The latter geometry and the same basis set and Hamiltonian were used to calculate ^{13}C shift tensors using GIAO.[15] This procedure resulted in a value of 60 ppm for $\delta_3-\delta_1$ of **6**.

At 250 K, the terminal allyl ^{13}C resonance of **6** consists of a broad line at 58.55 δ with a half width at half-height of 37.5 Hz. We assume that this resonance is the result of dynamic averaging of a 1:1 half spin uncoupled doublet of separation 60 ppm (4500 Hz at 70 054 G). Then, NMR line shape analysis[12,13] yields k_1 at 8.8×10^6 s^{-1} for the 1,3-sigmatropic shift of **6** at 250 K (Table 5). Recognizing an uncertainty of ±l0% in this calculated shift difference leads to an uncertainty of ±20% in the latter rate constant.

Compound 10. The organolithium moieties in **6** (dimer) and **10** (monomer) are identical with the exception that the ligand tether in **6** has one carbon, whereas in **10**, the tether is two

(14) Frisch, M. J.; Trucks, G. W.; Schlegel, H. B.; Scuseria, G. E.; Robb, M. A.; Cheeseman, J. R.; Zakrzewski, V. G.; Montgomery, J. A., Jr.; Stratmann, R. E.; Burant, J. C.; Dapprich, S.; Millam, J. M.; Daniels, A. D.; Kudin, K. N.; Strain, M. C.; Farkas, O.; Tomasi, J.; Barone, V.; Cossi, M.; Cammi, R.; Mennucci, B.; Pomelli, C.; Adamo, C.; Clifford, S.; Ochterski, J.; Petersson, G. A.; Ayala, P. Y.; Cui, Q.; Morokuma, K.; Malick, D. K.; Rabuck, A. D.; Raghavachari, K.; Foresman, J. B.; Cioslowski, J.; Ortiz, J. V.; Stefanov, B. B.; Liu, G.; Liashenko, A.; Piskorz, P.; Komaromi, I.; Gomperts, R.; Martin, R. L.; Fox, D. J.; Keith, T.; Al-Laham, M. A.; Peng, C. Y.; Nanayakkara, A.; Gonzalez, C.; Challacombe, M.; Gill, P. M. W.; Johnson, B. G.; Chen, W.; Wong, M. W.; Andres, J. L.; Head-Gordon, M.; Replogle, E. S.; Pople, J. A. *Gaussian 98*, revision A.1; Gaussian, Inc.: Pittsburgh, PA, 1998.

(15) (a) Wolinski, K.; Hilton, J. F.; Pulay, P. *J. Am. Chem. Soc.* **1990**, *112*, 8251. (b) Dodds, J. L.; McWeeny, R.; Sadlej, A. J. *Mol. Phys.* **1980**, *41*, 1419. (c) McWeeny, R. *Phys. Rev.* **1962**, *126*, 1028. (d) London, F. *J. Phys. Radium, Paris* **1937**, *8*, 397. (e) Ditchfield, R. *Mol. Phys.* **1974**, *27*, 789−807.

carbons long. Despite their different states of aggregation the NMR spectroscopic behaviors of **6** and **10** are very similar. At 292 K, the ^{13}C NMR of the terminal allyl carbons of **10** in diethyl ether solution consists of a single sharp peak at 51.62 δ. On cooling the sample, this resonance progressively broadened and disappeared into the baseline at 170 K. On further cooling, the compound precipitated from the solution. Throughout the entire temperature range 292−170 K, the two arms of the pendant ligand remained magnetically equivalent. In addition, there was no evidence for $^{13}C-^{7}Li$ spin coupling.

The above results are consistent with a fast 1,3-lithium sigmatropic shift in the monomer coupled with a fast equilibrium interconversion between monomer and a low, undetectable concentration of dimer. This system resembles **6** with the exception that the main component of **6** is the dimer and only a small fraction consists of monomer.

Chemical shift calculations for **10** were carried out in a fashion similar to those of **6**. The smaller size of monomeric **10** compared to the dimer **6** allowed use of the B3LYP and MPW1PW91 levels of theory in addition to RHF, all in conjunction with 6-311G* and 6-31+G* basis sets.[14] These methods gave very similar optimized geometries, which were confirmed to be stable energy-minimized structures with the usual freqeuency calculations. Using the latter geometry in conjunction with MPW1PW95 and basis set 6-31+G*, ^{13}C NMR shift tensors were calculated with GIA0,[15] giving a value for $\delta_3-\delta_1$ of 34 ± 3 ppm, similar to corresponding shift differences for monomeric **5**, **7**, **8**, **11**, **14**, and **15**. Assuming that the observed terminal allyl ^{13}C half width of 7.5 Hz at 250 K is the result of averging δ_3 with δ_1, we calculate k_1 for this shift to be 1.4×10^5 s^{-1}. An uncertainty in the above shift difference of ±9% results in an excursion of ±20% in the latter calculated rate constant (see Table 5).

Compound 13. This is the first of three allylic lithium compounds that incorporate a chiral auxiliary pendant ligand *N*[(*S*)-(2-methoxymethyl)-pyrolidino]−. These are intended to be used for future study of potentially enantioselective carbanion chemistry. Compound **13** was the starting material for preparing **14** and **15**. Though **13** is insoluble in all ethers tested, it did crystallize into two lithium-bridged dimers. Each of the (*S*)-(+)-2-methoxymethylpyrrolidino ligands is fully coordinated to lithium. Each lithium bears a η_3 relationship to one of the allyl moieties, as well as an interaction with one terminal carbon of the other allyl moiety even though the C−C allyl bond lengths are significantly different. Figure 7 shows the relationship of the two lithiums with respect to the allyl carbons and ligand sites. The remaining ligand structures and all the hydrogen atoms have been omitted for clarity. Interestingly, the two allyl bond lengths of **13** (weighted averages over two dimers), which are 1.415 (8) Å (C1−C2) and 1.368 (20) Å (C_2-C_3), are remarkably similar to those of **10**, 1.426 (2) Å (C_1-C_2) and 1.366 (2) (Å) (C_2-C_3), despite the different states of aggregation. Both are unsubstituted at the allyl termini, and both have the same ligand tether. However, the pendant ligands are different.

Compound 8. The solid-state structure of **8** confirms the ^{13}C shift assignments for the sample in diethyl ether-d_{10}. Well resolved spin coupling of 6.3 Hz between $^{13}C_1$ and ^{7}Li observed at 240 K is averaged on warming the sample due to bimolecular C−Li exchange. Averaging of $^{1}J(^{7}Li, ^{13}C)$ is also observed on cooling the sample below 240 K. The latter changes are diagnostic of ^{7}Li nuclear electric quadrupole-induced relaxation.[11]

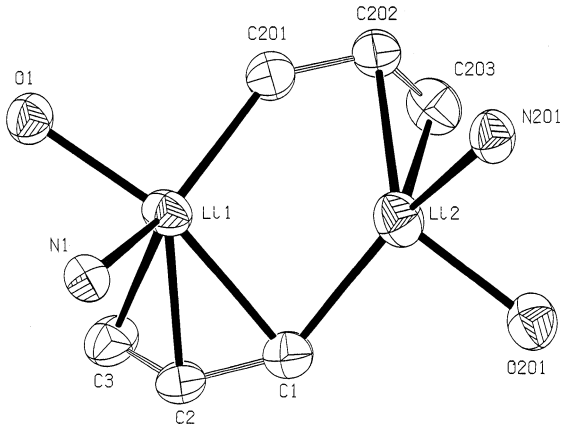

Figure 7. Relationship of lithiums with respect to the allyl carbons and coordinating ligand atoms in **13**. The remainder of the ligands and all hydrogen atoms have been omitted for clarity.

As reported previously[8b] between 270 and 330 K, there is progressive signal averaging of the two silyl methyl ^{13}C resonances due to a fast lithium 1,3 sigmatropic shift. NMR line shape analysis yields $\Delta H^{\ddagger} = 18.3 \pm 1.5$ kcal/mol and $\Delta S^{\ddagger} = 7 \pm 2$ eu for this process. That a single structure has been observed for this compound implies that the Li sigmatropic shift is accompanied by rotation around both allylic C−C bonds (see eq 2).

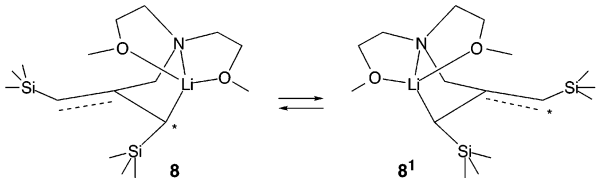

(2)

Preparation 12. In the solid state, the product of metalation of **20** by butyllithium as determined by X-ray crystallography is a single, partially localized, internally solvated monomer, described as structure **12**. The C−Si bonds of **12** lie close to the allyl plane. However, as shown below, in solution the above metalation product consists of a mixture of isomers. This mixture will be temporarily referred to as "**12**".

Carbon-13 NMR of "**12**" in diethyl ether-d_{10} between 170 and 292 K shows a clean equal doublet for each of O**C**H_2, O**C**H_3, and N**C**H_2C. Also, within this temperature range, the terminal allyl carbons exhibit resonances at 64.11 and 67.33 δ of approximately equal intensity, both of which consist of 1:1:1:1 equally spaced quartets with splittings of 4.6 and 4.1 Hz. These splittings are due to the effects of $^{13}C-^{7}Li$ spin coupling (see Figure 8).

With one exception, the ^{13}C NMR spectrum of "**12**" did not change between 170 and 292 K. On cooling the sample below 292 K the quartet structure at 64.11 and 67.33 δ due to $^{13}C_1-^{7}Li$ coupling progressively averaged. This is most likely due to ^{7}Li electric quadrupole-induced relaxation.[11]

Above 292 K with increasing temperature, ^{13}C NMR of the three equal doublets due to O**C**H_2, O**C**H_3, and N**C**H_2C progressively average to single lines at their respective centers.

^{13}C NMR results similar to those obtained for "**12**" in diethyl ether-d_{10} were observed using solutions of "**12**" in toluene-d_8 and benzene-d_6.

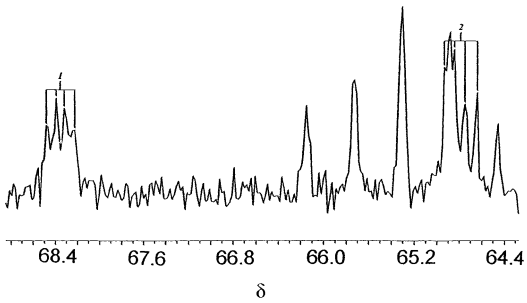

Figure 8. ^{13}C NMR (75.45 MHz) of **12** in diethyl ether-d_{10}, between 64.4 and 68.8 δ, 292 K.

Measurement of the freezing point depression of a solution of "**12**" in benzene established that the average molecular weight of "**12**" is identical to that of the crystallographic structure drawn above as **12**, i.e., the material is monomeric. Combining this result with the NMR data, it seems that "**12**" assumes the same structure or distribution of structures in all three media used for the NMR studies.

On the basis of the understood behavior of the other internally solvated allylic lithium compounds both previously published[8a−c] and described herein, we would like to propose that in solution, "**12**" consists of two stereoisomers, **12** and **29**, in almost equal concentrations that interconvert rapidly by means of a 1,3 lithium sigmatropic shift (see eq 6). The rate at temperatures down to 170 K is so fast as to preclude resolution of the terminal allyl ^{13}C resonances of **12** and **29**. By contrast, throughout the temperature range 170−292 K, rotation around the C_1-C_2 and C_2-C_3 bonds of **12** and **29**, bimolecular C−Li bond exchange, and transfer of coordinated lithium between faces of the allyl planes are *all slow* relative to the NMR time scale.

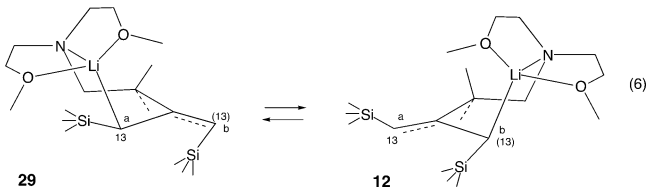

(6)

First, note that preparation "**12**" has ^{13}C in natural abundance. For convenience, the terminal allyl carbons are labeled as **a** and **b**. Consider the two equilibrating isotopomers **29-a**-^{13}C with **12-a**-^{13}C and **29-b**-^{13}C with **12-b**-^{13}C (see eq 6). Thus, of the two ^{7}Li bound ^{13}C resonances at 64.11 and 67.33 δ, one is the average shift of $^{13}C_a$ in **29-a**-^{13}C with $^{13}C_a$ in **12-a**-^{13}C. The ca. 4 Hz splitting of this resonance is the average of the one-bond $^{13}C_a-^7$Li coupling in **29-a**-^{13}C, ca. 8 Hz, with the very small or zero long-range $^{13}C_a-^7$Li coupling in **12-a**-^{13}C. Similar considerations apply to the averaged ^{13}C resonance of $^{13}C_b$ in **29-b**-^{13}C with that of ^{13}C in **12-b**-^{13}C. These two averaged ^{13}C resonances at 64.11 and 67.33 δ remain different because C−Li bimolecular exchange and rotation around the C_1-C_2 and C_1-C_3 bonds in **12** and **29** are both slow relative to the NMR time scale.

The magnitudes of the averaged terminal allyl ^{13}C shifts and of the splittings due to $^{13}C-^7$Li spin coupling in **12** and **29** are consistent with an equilibrium between two stereoisomers with closely similar concentrations. Thus, compounds **8**, **12**, and **29** have similar structures but with different ligand tethers. The average ^{13}C terminal allyl shift in **8** is 66.18 δ. This compares favorably with the corresponding proposed averaged values of 61.11 and 67.33 δ for the equilibrium between **12** and **29**.

Preparation 15. This material did not crystallize, but it did give rise to well-defined solution ^{13}C NMR spectra. The NMR data are consistent with an equilibrium between internally solvated monomeric allylic lithium compounds, proposed as **15** and **30**, in ratio of 2/1 (see eq 7), which interconvert by means of a 1,3 lithium sigmatropic shift. This process is slow relative to the NMR time scale up to 300 K. NMR parameters obtained from the solution of **15** with **30** are listed around the structure in Table 1 under "major" and "minor" components, respectively, since the shifts cannot be matched to the specific proposed structures.

The similarity of the NMR parameters of **15** and **30** to those of **10**−**12** and **14** supports partially delocalized structures for **15** and **30**. One terminal ^{13}C resonance each of **15** and **30** displays splitting due to $^{13}C-^7$Li spin coupling of 4.3 Hz at 65.47 δ for the minor component and 7.3 Hz at 56.34 δ for the major component. The second terminal ^{13}C shifts of **13** and **30** are both at 80.26 δ. The terminal allyl shifts of the major component are similar to those of **8** at 54.1 and 78.1 δ, implying that the major components of preparation **15** and **8** have similar electronic structures.

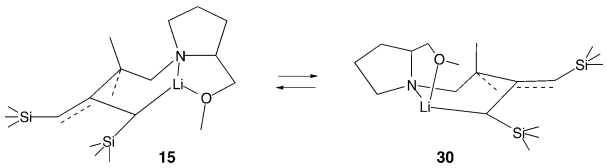

(7)

Compound 11. This compound did not crystallize. However, its NMR parameters are so similar to those of compounds whose structures were obtained via X-ray crystallography that one can assume that the structure of **11** resembles those of **8**, **10**, and **12**.

NMR of the ligand carbons was used to investigate the dynamics of face to face lithium transfer giving $\Delta H^{\ddagger} = 15 \pm 1$ kcal/mol and $\Delta S^{\ddagger} = +2 \pm 0.5$ eu, which is considerably slower than for compounds with a one-carbon tether for which $\Delta H^{\ddagger}$ is ca. 7 ± 0.5 kcal/mol. On the other hand, the dynamics of bimolecular C−Li exchange obtained from averaging of the $^{13}C-^7$Li spin coupling constant gives $\Delta H^{\ddagger} = 11 \pm 0.5$ kcal/mol and $\Delta S^{\ddagger} = -15 \pm 5$ eu (see Table 5).

Compound 14. This compound failed to crystallize in the pure state, but it did provide clean, well-resolved NMR spectra, which indicate a single molecular species. Impurities such as starting materials or oxidation products could not be detected among these NMR spectra. Clearly, the pendant chiral auxiliary is responsible for over 97% enantioselectivity in the formation of **14**.

Compound **14** exhibits one-bond $^{13}C-^7$Li coupling of 8.7 Hz and terminal allyl shifts of 37.22 δ (C_1) and 74.24 δ (C_3). These values are so similar to corresponding values for **5**, **7**, and **11** that one can assume that the silyl allyl moieties in all four species have similar electronic structures. The single silyl substituent at one allyl terminus appears to be responsible for the similar structural and NMR parameters among all four compounds. Meanwhile, ligand tethers and pendant ligands have far less influence on these parameters.

Averaging of the $^{13}C_1-^7$Li coupling with increasing temperature above 215 K yielded $\Delta H^{\ddagger}$ and $\Delta S^{\ddagger}$ for bimolecular C−Li

exchange of 6 ± 0.3 kcal/mol and −27 ± 5 eu, respectively (see Table 5).

Compound 9. Of all the compounds studied in this work, **9** is the most localized, with allyl bond lengths of 1.494 (7) Å (C_1-C_2) and 1.306 (8) Å (C_2-C_3) and ^{13}C shifts for C_1, C_2, and C_3 of 36.84, 171.2 and 118.8 δ, respectively. These parameters closely resemble those for a simple acyclic alkene.

With two silyl substituents at C_1 in **9** that are well separated by 135° on opposite sides of the allyl plane, the torsional angle $Li-C_1-C_2-C_4$ is just 30.03°. This arrangement minimizes potential steric interactions between the ligand and the TMS groups at C_1. It also places the C−Li bond closer to the allyl plane than in any of the other structures reported in this article. In this structure, the TMS groups at C_1 lie in very similar environments. In fact, just one sharp ^{13}C NMR peak is observed for each of $\mathbf{C}H_3O$, $\mathbf{C}H_2O$, and $N\mathbf{C}H_2C$ at temperatures down to 150 K.

A second consequence of the proximity of the C−Li bond to the allyl plane is that $^1J(^{13}C, ^7Li)$ is 15.7 Hz, that is, ca. twice that found for all other compounds described herein. Due to the small $Li-C_1-C_2-C_4$ angle in **9**, the C_{2s} contribution to the C_1-Li bond orbital would be larger than in the other internally solvated allylic lithium compounds we have studied.

General Conclusions. Comparison of the X-ray crystallographic and solution data show that the structures of our internally solvated allylic lithium compounds in the solid state and in solution must be very similar. In every case, the pendant ligand is fully coordinated to lithium and no solvent molecules are incorporated in the crystal structures. Most of these species are monomers in solution. Compound **6** is a dimer in both the solid state and in solution; **13** is a dimer in the solid state and insoluble in diethyl ether and in THF.

Lithium is localized near one of the allylic termini, and most of the compounds exhibit one-bond $^{13}C-^7Li$ or $^{13}C-^6Li$ spin coupling at low temperature. The existence of such coupling is consistent with the observed proximity of lithium to one of the allyl termini carbons.

Carbon-13 chemical shifts and bond lengths of the allylic moieties of the internally solvated allylic lithium compounds lie between those of the model species, the delocalized externally solvated ion-paired **1** and the unsolvated localized **2**.[5] Thus, the combined NMR and X-ray crystallographic data strongly support the proposition that these compounds are partially localized. Because the ligand tether is too short to place lithium normal to the center of the allyl plane, as in **1**, lithium is sited off the axis normal to the allyl plane at one of the carbon termini. This restricts the stereochemistry of coordination of lithium to the aberrant arrangements observed in the crystal structures and thereby stabilizes a partly delocalized allylic lithium compound, a new molecular species. It is tempting to consider that the proximity of Li^+ to a terminal allyl carbon is responsible for polarizing what would ordinarily be a delocalized anion into a partially localized one.

Prior to our report on **5**,[8a,b] spin coupling had not been observed between ^{13}C and ^6Li or ^7Li in any allylic lithium compound. The values reported herein for one-bond $^{13}C-^7Li$ spin coupling are much smaller than the common value of ca. 42 Hz observed for a wide variety of monomeric organolithium compounds (RLi, where R = alkyl, vinyl, aryl, alkynyl, and heterocyclic).[16a] The smaller and variable values of $^1J(^{13}C, ^7Li)$ for compounds **5**−**15** compared to the "common pattern" value of 42 Hz[16] may be due to the increased ionic character associated with the C−Li bonds in **5**−**15** compared to those for C−Li bonds in the above "common pattern" compounds, as has been recently proposed in a discussion on $^{13}C-Li$ spin coupling.[10a]

While the carbon lithium bonds in the species described in this article are most likely mainly ionic, the role of a small degree of C−Li covalency to these bonds and to the $^{13}C-^6Li$ and $^{13}C-^7Li$ coupling constants, respectively, cannot be eliminated. It is still uncertain. Although major advances have been made in the theory of scalar NMR coupling and in calculation of coupling constants, application of these methods to calculating $^{13}C-^6Li$ (or ^7Li) coupling constants has not been successful.

From the data in Table 2, it is evident that the degree of delocalization among **5**−**15** must be continuously variable. For example inspection of the data in Table 2 reveals in a qualitative way that as the torsional angle $Li-C_1-C_2-C_4$ decreases and the C−Li bond approaches the allyl plane, the difference between the allylic C_1-C_2 and C_2-C_3 bond lengths increases, as does the allylic ^{13}C chemical shift difference $\delta_3-\delta_1$. The limiting localized species is **9** with a $Li-C_1-C_2-C_4$ angle of −30.3°. Its allylic ^{13}C shifts and bond distances closely resemble those of a simple alkene. Compound **9** also exhibits the largest $^{13}C-^7Li$ coupling constant reported herein, 15.9 Hz. This is most likely due to the increased "S" character associated with the C−Li bond in **9** when compared to those in the other compounds, **5**, **7**, **8**, **11**, **14**, and **15**.

Averaging of the $^{13}C-^7Li$ or $^{13}C-^6Li$ coupling constants with increasing temperature is necessarily due to bimolecular C−Li exchange. This requires that the mechanism for the exchange process proceeds via a dimeric transition state that is most likely preceded by a dimeric intermediate. In fact, two of the compounds in Table 1, **6** and **13**, are dimers. Thus, it is reasonable to assume that dimeric intermediates are energetically accessible to our internally solvated allylic lithium compounds, which are monomeric in their ground states.

Considering the wide variety of structures we have investigated, the activation enthalpies we have determined for bimolecular C−Li exchange are remarkably similar. They all fall within the range 11−12 kcal/mol. A species as different as the internally solvated benzylic lithium compound, **31**, also exhibited a $\Delta H^{\ddagger}$ for C−Li exchange of 11 kcal/mol for bimolecular C−Li exchange.[8d] These results suggest that the rate-determining step for bimolecular C−Li exchange involves dechelation of lithium from the pendant ligand.

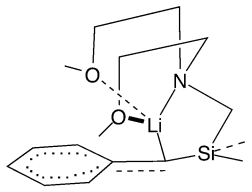

31

Dynamics of configurational inversion are obtained from NMR line shape analysis of the pendant ligand resonance. It is a first-order process and results overall from transfer of coordinated lithium between faces of the allyl plane. The rates

(16) (a) Bauer, W.; Winchester, W. R.; Schleyer, P. v. R. *Organometallics* **1997**, *6*, 2371−2379. (b) Bauer, W.; Griesinger, C. *J. Am. Chem. Soc.* **1993**, *115*, 10871. (c) Lambert, C.; Schleyer, P. v. R. *Angew. Chem., Int. Ed. Engl.* **1994**, *33*, 1129.

depend on the ligand tether with ca. $\Delta H^{\ddagger}$ of 6.5 ± 0.5 kcal/mol for a one-carbon tether and 15 ± 1 kcal/mol for a two-carbon tether, in the case of compound **11**. Configurational inversion also accompanies fast lithium sigmatropic shifts in symmetrical internally solvated allylic lithium compounds.

By contrast to the fairly uniform activation parameters for inversion and bimolecular C−Li exchange, 1,3 lithium sigmatropic shifts take place at remarkably different rates. The dynamics of this sigmatropic shift can only be investigated in the cases of compounds **6**, **8**, **10**, **12**, and **15**. These are symmetrical species that are either unsubstituted at the allyl termini or possess one TMS group at each terminal allyl carbon.

As seen in Table 5 at 250 K, relative to the NMR time scale, the 1,3 lithium sigmatropic shift for **12** ⇄ **29** is too fast to measure, while that of **15** ⇄ **30** is too slow to measure. Between the latter two extremes are **8** with a k_1 of 1 s^{-1} and **6** and **10** whose lithium sigmatropic shifts are estimated to be faster than that of **8** by factors of ca. 10^7 and 10^5, respectively.

Modeling of these latter compounds indicates that differences among steric interactions that accompany the Li sigmatropic shifts may be responsible for the wide variations among the rates. Thus, the unsubstituted compounds **6** and **10** offer minimum constraints to rearrangement. However, the shift in **8** would be hindered by the proximity of the tethered ligand to the silyl substituents. The longer tether in **12** reduces the latter steric constraints. By contrast to the **29** ⇄ **12** interconversion (eq 6), the steric interactions that accompany **15** ⇄ **30** would be far more severe due to the proximity of the −Li−N−CH−CH_2O− moiety to the allyl surface.

In summary, it has been established that, among several internally solvated allylic lithium compounds, the ligand tether is too short to place coordinated lithium normal to the center of the allyl plane as in **1**. Instead, coordinated lithium is placed closer to one of the terminal allyl carbons. This polarizes what would otherwise be a delocalized allyl anion to a partly localized species. Dynamic behavior associated with inversion, C−Li exchange, and 1,3 lithium sigmatropic shifts has also been uncovered.

Experimental Section

General manipulations of organometallic compounds were carried out under an atmosphere of argon or nitrogen. Solvents were dried over Na/K alloy. NMR spectra were obtained using Bruker AM250 or Bruker Avance 300 equipment.

Preparation of Allylic Lithium Samples for Crystallography. Typical Procedure: 2-Bis(2-methoxyethyl)aminomethyl-1-trimethylsilylallyllithium (5). Under an argon atmosphere at 0 °C, butyllithium (1.25 mL, 1.6 M, 2 mmol) in hexane was slowly added to a solution (0 °C) of 2-bis(2-methoxyethyl)aminomethyl-3-trimethylsilyl-1-propene (0.52 g, 2 mmol) in 10 mL of hexane. The mixture was allowed to warm to room temperature and then stirred for 1 h. The volume of the reaction mixture was reduced to 5 mL under vacuum. Crystals developed after standing the sample overnight at room temperature. Toluene has also been used in these crystallization procedures.

2-Bis(2-methoxyethyl)aminomethylallyllithium, Crystals 5. Methyllithium (1.9 mL, 1.4 M, 2.2 mmol) in ether was added to 2-bis(2-methoxyethyl)aminomethylpropene (0.5 g, 2,7 mmol) in 5 mL of THF at 0 °C. After addition of the CH_3Li, the solution was allowed to warm to room temperature slowly and then stirred for 15 min. The volume was reduced to 3 mL. Colorless crystals developed after storing the sample at room temperature overnight.

X-ray Crystallography: General Procedures. A sample of the crystalline material was removed from the mother liquor using standard Schlenk techniques and coated with Paratone N, an inert oil. Crystals were handled under oil under a microscope. Suitable crystals were then mounted at the end of a glass fiber in a drop of Paratone N and then shock cooled on the diffractometer. All data were collected at 173 K on an Enraf-Nonius diffractometer with a CCD area detector using graphite monochromatic Mo Kα radiation ($\lambda = 0.71073$ Å). Structures were solved by direct methods with SHELXS-97[17] and were refined by full matrix least squares procedures on F^2 using SHELXL-97.[18] All non-hydrogen atoms were refined anisotopically. Allylic and vinylic hydrogen atom positions were taken from the difference electron density map and refined freely. Other hydrogen atoms were positioned at ideal geometries, and a riding model was employed in the refinement. The denoted *R* values are defined as follows:

$$R_1 = \sum||F_o| - |F_c||\Big/\sum|F_o|$$

$$wR_2 = \{\sum w(F_o^2 - F_c^2)^2/\sum w(F_o^2)^2\}^{1/2};$$
$$w = 1/\{\sigma^2(F_o^2) + (g1*P)^2 + g2*P\};\ P = (F_o^2 + 2F_c^2)/3$$

Further details on structure investigation can be obtained from the Director of the Cambridge Crystallographic Data Centre, 12 Union Road, GB-Cambridge C132 1 EZ, UK, by quoting the full journal reference.

Allylic Lithium Compounds, General Procedure for NMR Samples. Butlyllithium in hexane (3.13 mL, 1.6 M, 5 mmol) was added slowly by syringe at 0 °C to a solution of the appropriate substituted propene (5 mmol) in 10 mL of freshly distilled dry, oxygen-free diethyl ether. After this addition was complete, the mixture was allowed to warm to room temperature and then stirred for 1 h. An aliquot (1 mL) of this solution was transferred into an NMR tube with attached joint and straight bore stopcock. All volatile material was removed in vacuo and then replaced by deuterated solvent, diethyl ether-d_{10} or THF-d_8. The latter was distilled from sodium over the vacuum line into the NMR tube. The sample tube was degassed via three freeze−thaw cycles and then sealed off frozen with pumping.

Silylation of Allylic Lithium Compounds: General Procedure. A freshly prepared sample of an allylic lithium compound (5 mmol) was cooled to −78 °C, and chlorotrimethylsilane (0.54 g, 0.64 mL, 5 mmol) was added slowly by syringe. Upon completion of the addition, the mixture was allowed to warm to room temperature. The onset of reaction at −40 °C was indicated by precipitation of LiCl. The mixture was stirred for an additional 1 h. Saturated aqueous $NaHCO_3$ (10 mL) was added to remove excess chlorotrimethylsilane. The aqueous phase was extracted twice with 10 mL diethyl ether. The combined nonaqueous phases were dried over Na_2SO_4 the solvent was removed, and the residue was distilled.

Allylic Lithium Samples for NMR Study. At 0 °C under an atmosphere of argon, *n*-butyllithium (3.13 mL, 1.6 M, 5 mmol) in hexane was slowly added to a solution of the appropriate substituted alkene (5 mmol) in 10 mL of freshly distilled dry, oxygen-free diethyl ether. Upon complete addition, the reaction mixture was allowed to warm to room temperature and then stirred for 1 h. A 1 mL aliquot of this solution was syringed into a 5 mm OD NMR tube equipped with an attached joint and a 2 mm straight bore stopcock. All volatile material was removed in vacuo and replaced by diethyl ether-d_{10} or THF-d_{10}. The latter solvent was distilled from sodium over the vacuum line into the NMR tube. The loaded sample was degassed via three freeze−thaw cycles and then sealed off frozen with pumping.

Freezing Point Depression of 6 in Benzene. A solution of butyllithium in hexane (1.25 mL, 1.6 M, 2 mmol) at 0 °C under argon was slowly added to **16** (0.37 g, 2 mmol) in 5 mL of diethyl ether. The mixture was allowed to warm to room temperature and then stirred for 1 h. All volatile components of this reaction mixture were removed in vacuo (10^{-3} Torr), and the residue was dissolved in 12.2 g of dry, oxygen-free benzene. The resulting solution was syringed into a dry,

(17) Sheldrick, G. M. *Acta Crystallogr., Sect A* **1990**, *481*, 467.
(18) Sheldrick, G. M. *SHELXL-97, Program for Crystal Structure Refinement*; University of Göttingen: Göttingen, 1997.

oxygen- and moisture-free 50 mL insulated flask equipped with a Beckman thermometer and mechanical stirrer. The above-described benzene solution showed a freezing point depression of 0.36 ± 0.03 °C compared to pure benzene. This corresponds to a state of aggregation of 2.17 compared to benzene. Assuming all of the starting material is converted to **6** and using the freezing point depression of 49 °C for 1 mol of solute in 100 g of benzene, the above freezing point depression corresponds to a state of aggregation of 2.23.

2-(Bis(2-methoxyethyl)aminomethyl)-1,3,3-tris(trimethylsilyl)-1-propene, (17). At 0 °C and under an atmosphere of argon, *n*-butyllithium (2.3 mL, 2.5 M, 57 mmol) in hexane was slowly added to **16** (3.63 g, 19 mmol) in 25 mL of diethyl ether. After stirring for 30 min, the mixture was cooled to −78 °C and chlorotrimethylsilane (6.2 g, 7.5 mL, 57 mmol) was added dropwise. After completion of the addition, the mixture was allowed to warm to room temperature and then stirred for 1 h. The mixture was treated with 30 mL of saturated Na_2CO_3 (aq); the phases were separated, and the aqueous phase was extracted with diethyl ether (3 × 20 mL). The combined organic layers were washed with NaCl (aq) (2 × 20 mL) and dried over Na_2CO_4. Removal of solvent and distillation of the residue gave 6.15 g of the title compound in 80% yield, bp 99−100 °C at 0.05 Torr. ^{1}H NMR ($CDCl_3$, 250 MHz, δ): 0.034 (s, 18), 0.048 (s, 9), 1.728 (s, 1), 2.584 (t, 4, ^3J = 6.2 Hz), 2.988 (s, 2), 3.270 (s, 6), 3.403 (t, 4, ^3J = 6.2 Hz), 4.927 (s, 1). ^{13}C NMR ($CDCl_3$, 75 MHz, δ): 0.37, 0.53, 25.40, 52.95, 58.07, 62.86, 70.97, 124.10, 157.52.

4-Bis(2-methoxyethyl)amino-3,3-dimethyl-2-trimethylsilylmethyl-1-butene, (19). At 0 °C under an atmosphere of argon, *n*-butyllithium (8 mL, 2.5 M, 20 mmol) in hexane was added dropwise to **18** (4.59 g, 20 mmol) in 20 mL of diethyl ether. The resulting reaction mixture was treated with trimethylchlorosilane (2.54 mL, 20 mmol) at −78 °C. The usual workup afforded 3.48 g of the title compound in 58% yield, bp 92−97 °C at 0.5 Torr. ^{1}H NMR ($CDCl_3$, 250 MHz, δ): −0.014 (s, 9), 0.935 (s, 6), 1.451 (s, 2), 2.377 (s, 2), 2.644 (t, J = 6.5 Hz), 3.371 (t, J = 6.5 Hz), 4.579 (s, 1), 4.730 (s, 1). ^{13}C NMR ($CDCl_3$, 75 MHz, δ): −0.49, 21.35, 25.23, 41.39, 55.81, 58.68, 65.61, 71.60, 108.19, 152.91.

4-*N*-Bis(2-methoxyethyl)amino-3,3-dimethyl-1-trimethylsilyl-2-trimethylsilylmethyl-1-butene (20). At 0 °C under an atmosphere of argon, *n*-butyllithium (3.4 mL, 2.5 M, 85 mmol) in hexane was added dropwise to **18** (6.5 g, 28.3 mmol) in 50 mL of diethyl ether. The reaction was allowed to warm to room temperature with stirring over 1 h. After the reaction mixture was cooled to −78 °C, trimethylchlorosilane (9.23 g, 10.8 mL, 85 mmol) was slowly added. Reaction was observed on warming the mixture to −40 °C. The workup described above gave 8.25 g of the title compound in 78% yield, bp 120 °C at 0.2 Torr. ^{1}H NMR ($CDCl_3$, 250 MHz, δ): −0.044 (s, 9), 0.002 (s, 9), 0.867 (s, 6), 1.701 (s, 2), 2.281 (s, 2), 2.551 (t, 4, J = 6.7 Hz), 3.176 (s, 6), 3.268 (t, 4, J = 6.7 Hz), 5.031. ^{13}C NMR ($CDCl_3$, 75 MHz, δ): 0.59, 24.21, 26.29, 43.00, 55.88, 58.67, 67.90, 71.66, 119.47, 163.50.

Freezing Point Depression of 2-(2-Methyl-3-bis(2-methoxyethylethyl)amino)-2-propyl)-1,3-bis(trimethylsilyl)allyllithium (12). At 0 °C under an atmosphere of argon, *n*-butyllithium (1.56 mL, 1.6 M, 2.5 mmol) in hexane was added dropwise to **20** (0.93 g, 2.5 mmol) in 5 mL of hexane. The reaction mixture was brought to room temperature and stirred for 30 min. All volatile material was removed in vacuo (0.2 Torr), and the residue was dissolved in 8.6 g of benzene. The resulting solution was syringed into a flame-dried, argon-filled 50 mL insulated flask equipped with a Beckman thermometer and a mechanical stirrer. During the experiment, a steady flow of argon was maintained to ensure an inert atmosphere. This sample showed a freezing point depression of 1.4 °C versus pure benzene, indicating a state of aggregation of 1.02.

***N*-((*S*)-(+)-(2-Methoxymethyl)pyrollidino)-2,2,3-trimethyl-but-3-enoic Amide (22).** To carboxylic acid **21** (6.41 g, 50 mmol) was added dropwise thionyl chloride (7.16 g, 60 mmol). The mixture was heated to 85 °C for 1 h. Excess thionyl chloride was removed by distillation and the remaining mixture was chilled to 0 °C. Free amine (*S*)-(+)-2-methoxy-methylpyrollidine (11.4 g, 100 mmol) was added, and the mixture was stirred for 3 h at room temperature. Then, 15 mL of water was added, and the layers were separated. The aqueous layer was extracted with diethyl ether (3 × 15 mL), and the combined nonaqueous extracts were washed with $NaHCO_3$ (aq) and then dried over $MgSO_4$. Removal of solvent gave 9.4 g of the title compound in 83% yield. The product was 99% pure by chromatographic analysis. ^{1}H NMR ($CDCl_3$, 250 MHz, δ): 1.236 (s, 3), 1.241 (s, 3), 1.645 (s, 3), 1.85 (bm, 4), 3.23 (m, 1), 3.249 (s, 3), 3.35 (m, 1), 3.47 (m, 2), 4.788 (bd, 2). ^{13}C NMR ($CDCl_3$, 63 MHz, δ): 19.70, 25.02, 25.18, 25.30, 26.56, 47.41, 48.43, 58.74, 72.30, 77.00, 109.70, 148.76, 174.02.

Treatment of the above aqueous solution with KOH (4 g) followed by extraction into ether recovered 4.8 g of the unreacted amine.

4-*N*-((*S*)-(+)-(2-Methoxymethyl)pyrrolidino-2,3,3-trimethyl-1-butene (23). A solution of amide **22** (9.4 g, 42 mmol) in 20 mL of dry THF was slowly dropped into a suspension of $LiAlH_4$ (1.3 g, 45 mmol) in 100 mL of THF. After refluxing this mixture overnight, 15 mL of 15% NaOH (aq) was added, which produced a white precipitate. Separation of the liquid phase followed by removal of solvent yielded 8.7 g of the title amine in 90% yield. ^{1}H NMR ($CDCl_3$, 250 MHz, δ): 0.985 (s, 3), 1.042 (s, 3), 1.52 (m, 1), 1.66 (m, 2), 1.726 (s, 3), 1.78 (m, 1), 2.180 (m, 1), 2.389 (d, 1, ^2J = 13.1 Hz), 2.57 (m, 1), 2.618 (d, 1, ^2J = 13.1 Hz), 3.150 (m, 2), 3.303 (s, 3), 3.340 (m, 1), 4.706 (m, 2). ^{13}C NMR ($CDCl_3$, 64 MHz, δ): 19.85, 23.78, 25.91, 26.31, 28.35, 40.48, 56.86, 58.90, 65.23, 66.31,77.00, 109.68, 152.45.

4-*N*-((*S*)-(+)-(2-methoxymethyl)pyrrolidino)-3,3-dimethyl-2-trimethylsilylmethyl-1-butene (24). At 0 °C under an argon atmosphere, *n*-butyllithium in hexane (12 mL, 2.5 M, 30 mmol) was added dropwise to compound **23** (6.34 g, 30 mmol) in 26 mL of diethyl ether. The reaction mixture was warmed to room temperature, stirred for 3 h, and then reacted at −78 °C with trimethylchlorosilane (3.26 g, 3.8 mL, 30 mmol). Workup yielded 6 g of the title compound in 71% yield, bp 91 °C at 0.2 Torr. ^{1}H NMR ($CDCl_3$, 250 MHz, δ): 0.019 (s, 9), 0.952 (s, 3), 1.023 (s, 3), 1.55−1.90 (m, 4), 2.2 (m, 1), 2.386 (d, 1, ^2J = 13.1 Hz), 2.57 (m, 1), 2.597 (d, 1, ^2J = 13.1 Hz), 3.15 (m, 1), 3.313 (s, 3), 3.37 (m, 1), 4.769 (d, 1, ^2J = 1.2 Hz), 4.595 (d, 1, J = 1.2 Hz). ^{13}C NMR ($CDCl_3$, 64 MHz, δ): −0.419, 21.37, 23.83, 25.78, 26.05, 28.45, 41.29, 57.14, 58.95, 65.36, 66.40, 77.09, 107.90, 153.86.

4-*N*-(*S*)-(+)-(2-Methoxymethyl)pyrolidino)-3,3-dimethyl-1-trimethylsilyl-2-trimethyl-silylmethyl-1-butene (25). At 0 °C under an argon atmosphere, *n*-butyllithium in hexane (10 mL, 16 mmol, 1.6 M) was added with stirring to **24** (4.56 g, 16 mmol) in 10 mL of diethyl ether. The reaction mixture was warmed to room temperature and stirred for an additional 3 h, and then it was reacted at −78 °C with trimethylchlorosilane (1.47 g, 2 mL, 16 mmol). Workup yielded 5.01 g of the title compound. ^{1}H NMR ($CDCl_3$, 250 MHz, δ): 0.065 (s, 18), 0.980 (s, 3), 1.028 (s, 3), 1.4−1.7 (b, 4), 1.833 (s, 2), 2.189 (q, 1), 2.393 (d, 1, ^2J = 13.3 Hz), 2.53 (m, 1), 2.565 (d, 1, ^2J = 13.3 Hz), 3.104 (m, 2), 3.314 (s, 3), 3.358 (q, 1), 5.151 (s, 1). ^{13}C NMR ($CDCl_3$, 63 MHz, δ): 0.59, 0.65, 23.90, 24.44, 26.64, 27.52, 28.56, 42.71, 57.33, 58.96, 65.28, 68.89, 77.12, 119.10, 164.14.

Acknowledgment. This research was generously supported by the National Science Foundation Grant No. CHE 0077605 and by the Newman Chair. R.F. thanks the Deutscher Akademischer Austausch Dienst for Fellowship support. We thank Dr. Charles Cottrell, Central Campus Instrumentation Center, for untiring technical assistance. We thank Dr. Judith Gallucci for clarifying some issues related to the X-ray crystallographic data.

Note Added after ASAP. In the version posted 3/4/04, ref 7 was incorrect. The version posted 3/9/04 and the print version are correct.

Supporting Information Available: Crystallographic data and NMR spectra. This material is available free of charge via the Internet at http://pubs.acs.org.

JA030370Y